Electronic Supplementary Material (ESI) for Faraday Discussions.

Supporting Information

Polymeric Integration of Structure-Switching Aptamers on Transistors for Histamine Sensing

Bajramshahe Shkodra,[1,3] Mattia Petrelli,[1] Kyung-Ae Yang,[2] Anna Tagliaferri,[1] Paolo Lugli,[1] Luisa Petti,[1] Nako Nakatsuka[3]

[1]Faculty of Science and Technology, Free University of Bozen-Bolzano, Piazza Università 1, 39100 Bozen, Italy

[2]Center for Innovative Diagnostic and Therapeutic Approaches, Department of Medicine, Columbia University, New York, New York 10032, United States

[3] Laboratory of Biosensors and Bioelectronics, Institute for Biomedical Engineering, ETH Zürich, CH-8092, Switzerland

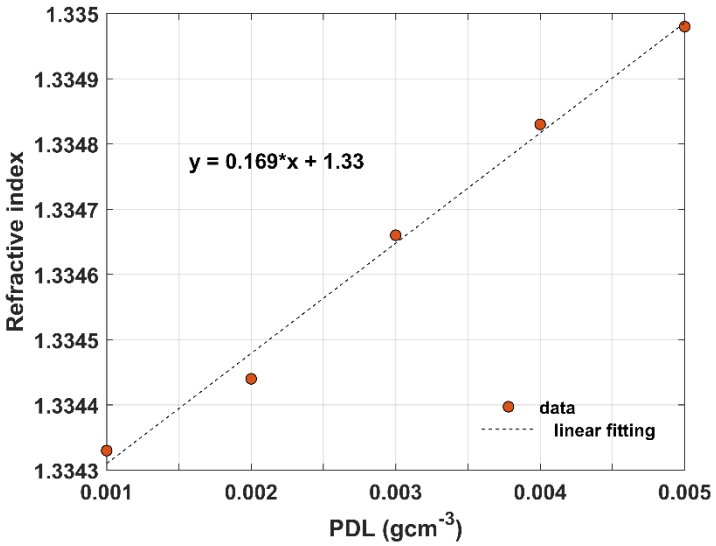

Figure S1. Calibration curve presenting poly-*D*-lysine (PDL) concentration in gcm^{-3} *versus* the corresponding measured refractive index. The slope of the calibration curve represents the refractive index increment for PDL.

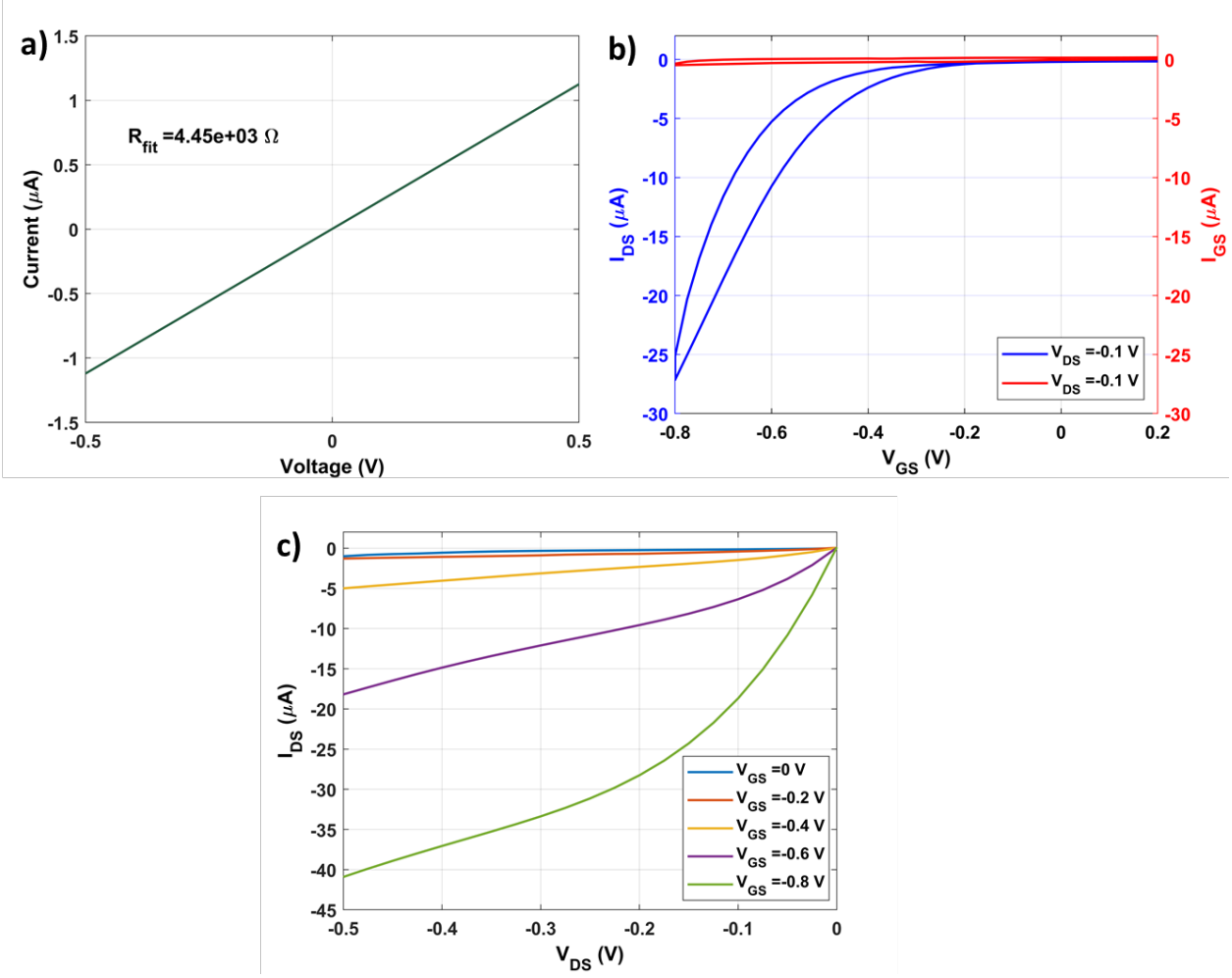

Figure S2. Electrical characterization of the devices. a) Source-drain resistance measured for electrolyte-gated carbon nanotube field-effect transistors (EG-CNTFETs) was ≤ 10 kΩ. b) The transfer characteristic shows an I_{ON}/I_{OFF} = 630 ± 245 A/A and threshold voltage of -0.46 ± 0.05 V. The gate current remained at least two orders of magnitude lower than the drain current during the entire sweep. c) The output characteristics were recorded varying the V_{DS} from 0 V to -0.5 V for different values of V_{GS} from +0.2 V to -0.8 V, with -0.2 V steps.

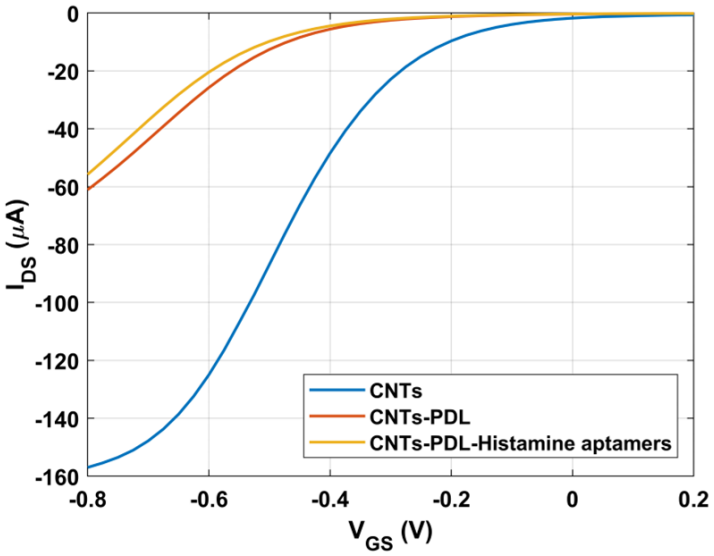

Figure S3. Representative transfer characteristics taken after each functionalization step of electrolyte-gated carbon nanotube field-effect transistors (EG-CNTFETs). Measurements were performed in 1x PBS. The poly-*D*-lysine (PDL) attachment on the nanotubes acts as an insulator and therefore a decrease in the drain-source current (I_{DS}) is observed. The additional layer of aptamers likely serves as a further insulating polymer layer, leading to a further I_{DS} decrease.

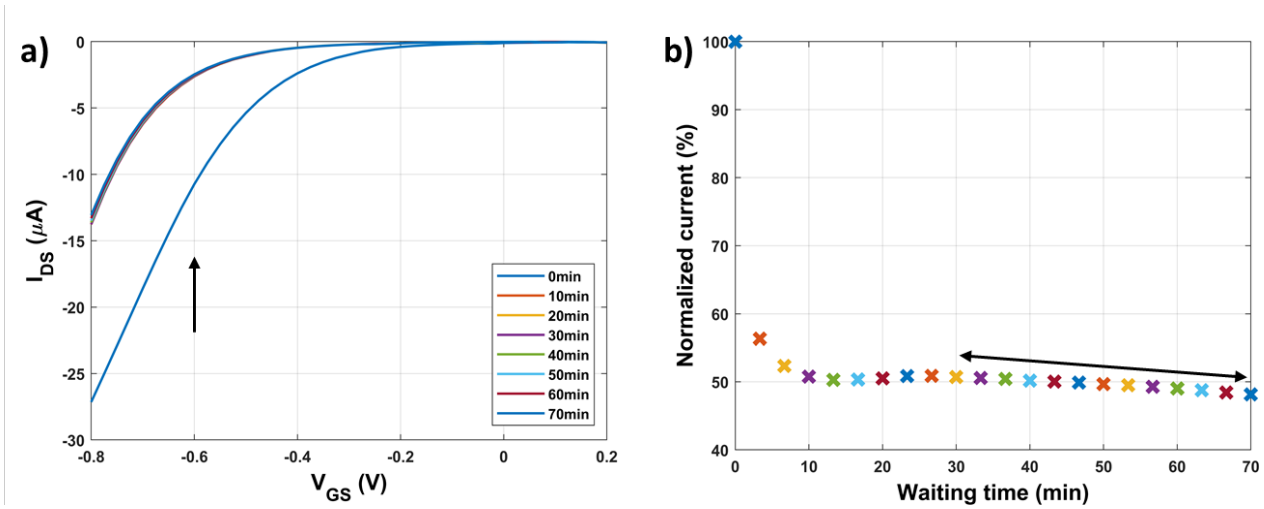

Figure S4. Monitoring electrolyte-gated carbon nanotube field-effect transistor (EG-CNTFET) time stability. a) Transfer characteristics recorded in 1x PBS for 70 min and b) the normalized current versus the waiting time. The response of the device (*i.e.,* the I_{DS} value at V_{GS} = -0.8 V) initially jumps after 10 min in the ionic solution and then remained stable after 30 min. Then, the I_{DS} showed a linear decrease in absolute value (*i.e.,* for this specific device, a decrease of 17.5 nA/min with a coefficient of determination of 98.65%). It was hence possible to subtract this linear trend from the response of the devices to different concentrations of histamine (calibrated response).

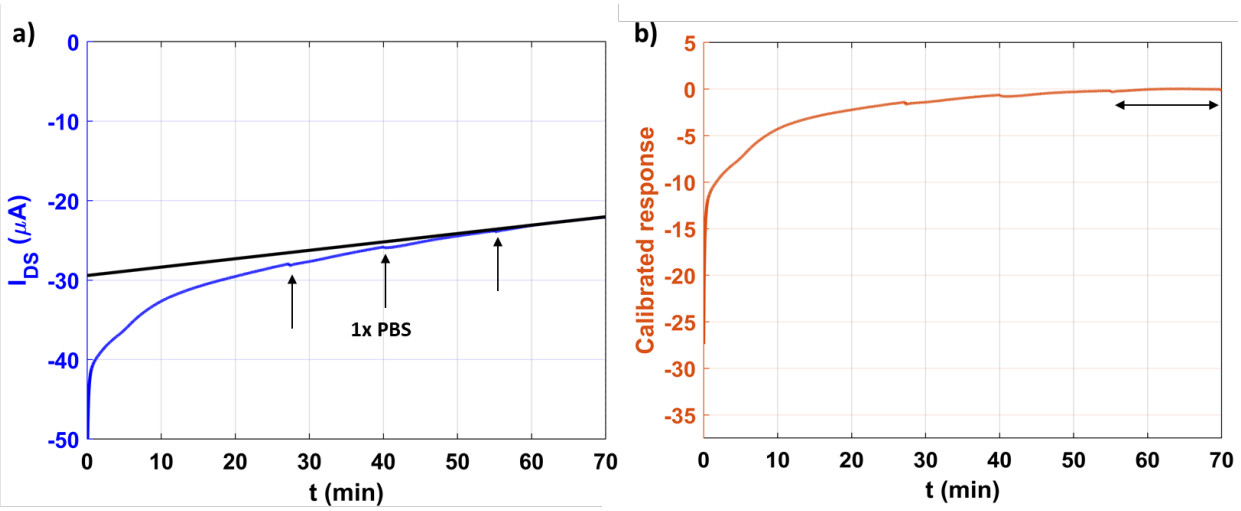

Figure S5. Monitoring electrolyte-gated carbon nanotube field-effect transistor (EG-CNTFET) time stability. a) The I_{DS} current *vs*. time measurements recorded in 1x PBS for 70 min. To ensure that injection does not affect the device response, 1x PBS was always injected into the system three times prior to injection of histamine (indicated with black arrows). b) The calibrated response of the device remained stable after 60 min.

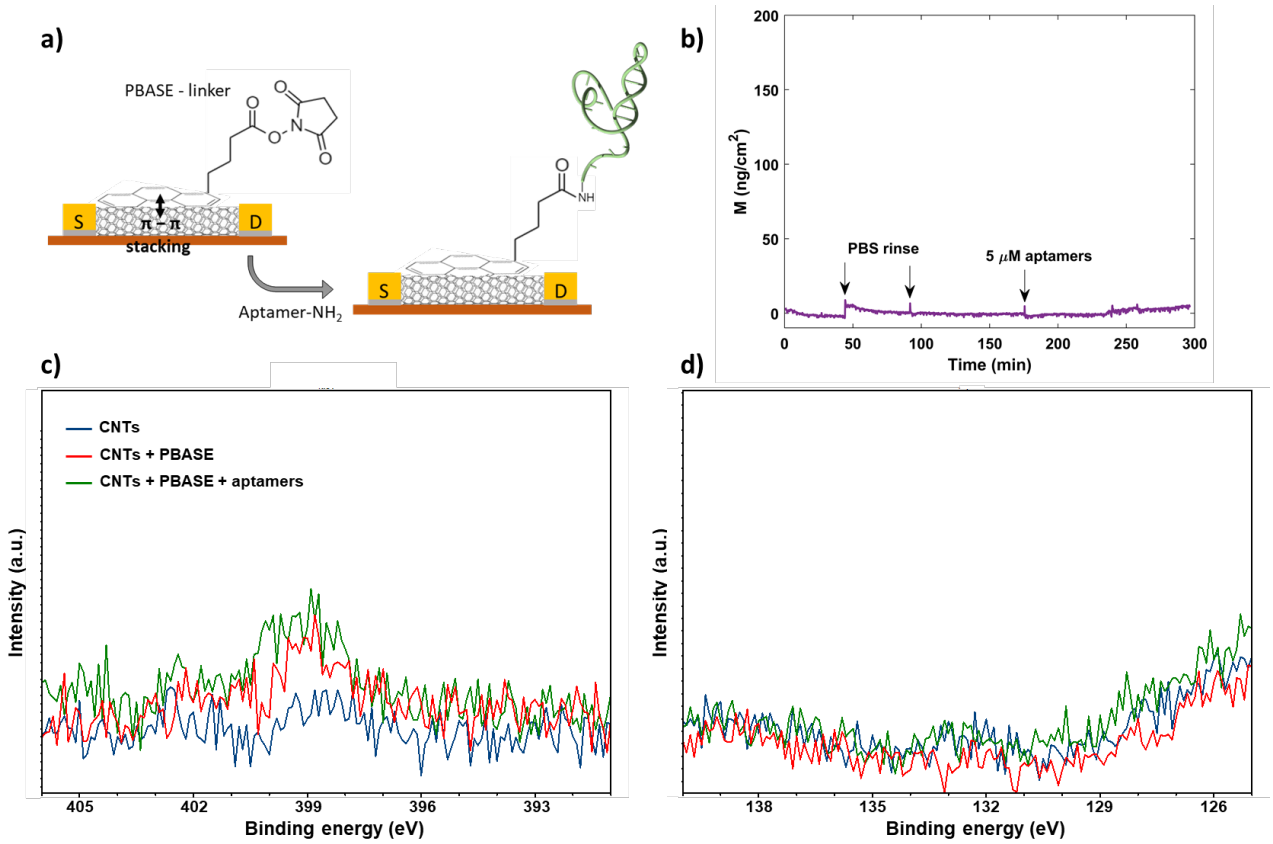

Figure S6. a) Schematic of the pyrene functionalization strategy with the benzene rings of 1-pyrenebutyric acid N-hydroxysuccinimide ester (PBASE) attaching to the carbon nanotubes (CNTs) due to π-π stacking, while the N-hydroxysuccinimide ester remains free to react with the primary amines on the aptamers. b) Changes in the mass density during the adsorption process obtained by optical waveguide lightmode spectroscopy (OWLS) on a CNT-coated waveguide. Negligible changes were observed upon incubation of the histamine aptamers to PBASE-modified waveguide surfaces. c) X-ray spectroscopy spectra for the N 1s peak intensities and d) the P 2p peak intensities for bare CNTs (blue line), CNT-PBASE (red line), and post-aptamer functionalization (green line). Negligible changes were observed for both the N 1s and P 2p peak intensities compared to substrates functionalized with the polymeric layer-by-layer assembly (Main text, Figure 2 b,c).

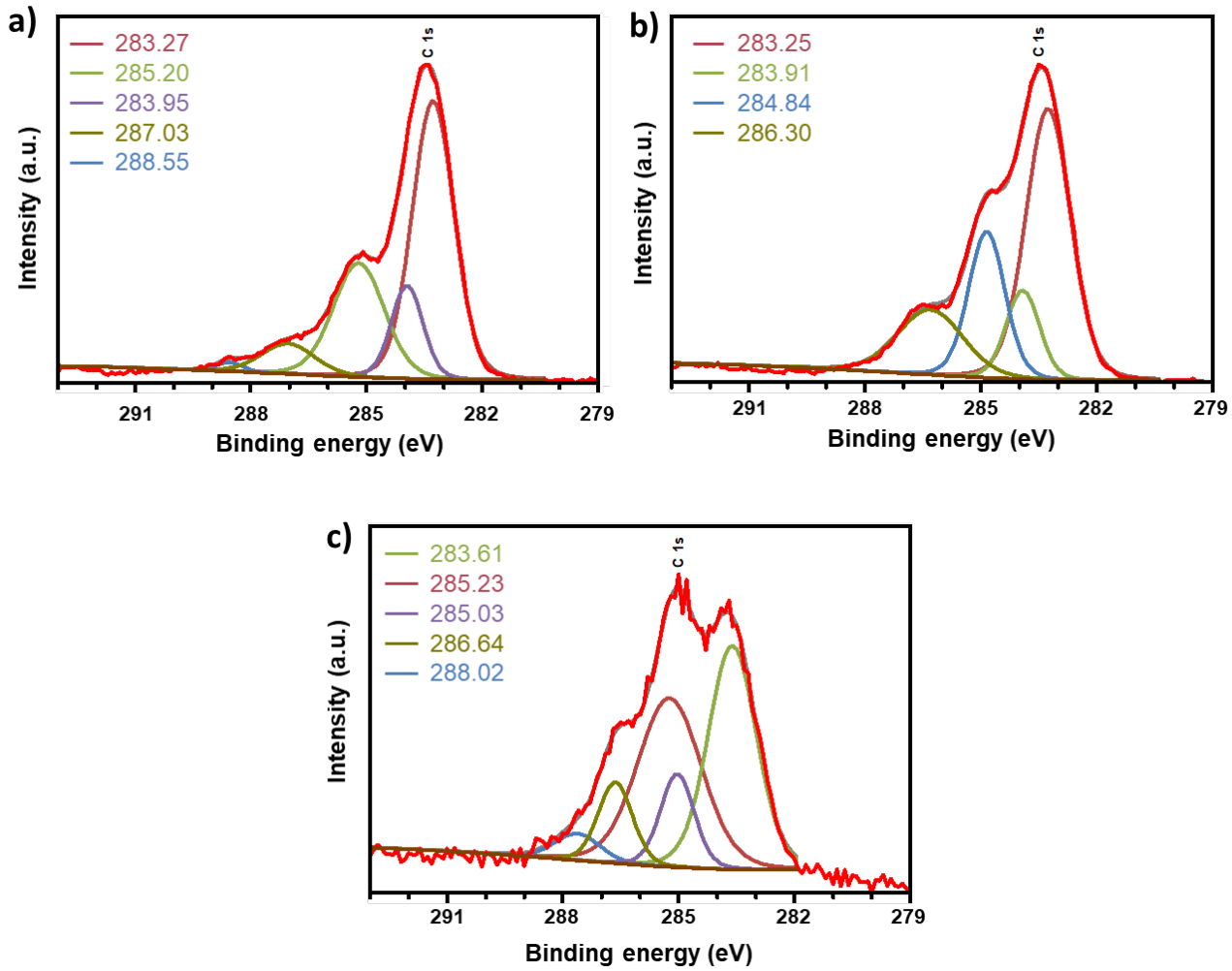

Figure S7. High-resolution X-ray photoelectron spectroscopy (XPS) C 1s spectra for a) bare CNTs, b) PDL-coated CNTs, and c) aptamer-modified CNTs.

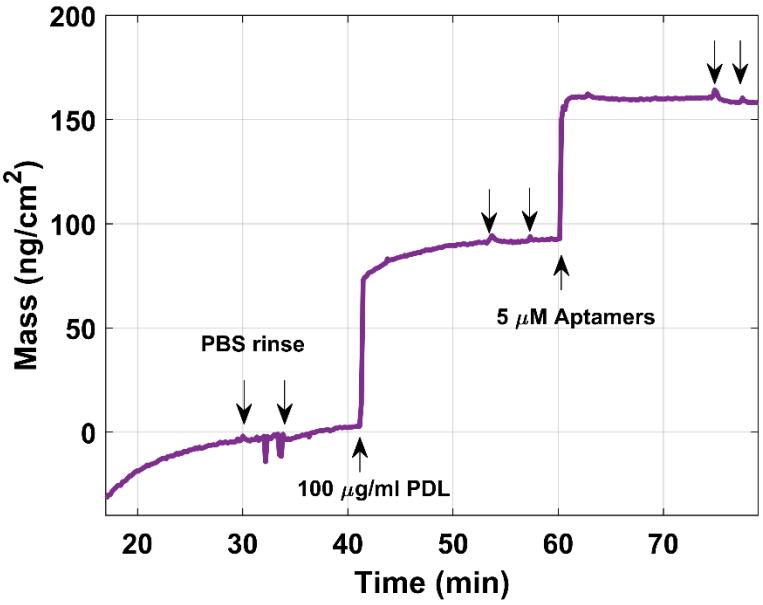

Figure S8. Changes in the mass density during the adsorption process obtained by optical waveguide lightmode spectroscopy (OWLS) on a bare waveguide. Addition of poly-*D*-lysine (PDL) and subsequent injection of aptamers resulted in an increase in the adsorbed mass. Downward facing arrows indicated phosphate buffered saline (PBS) rinsing steps to ensure robust layer formation.

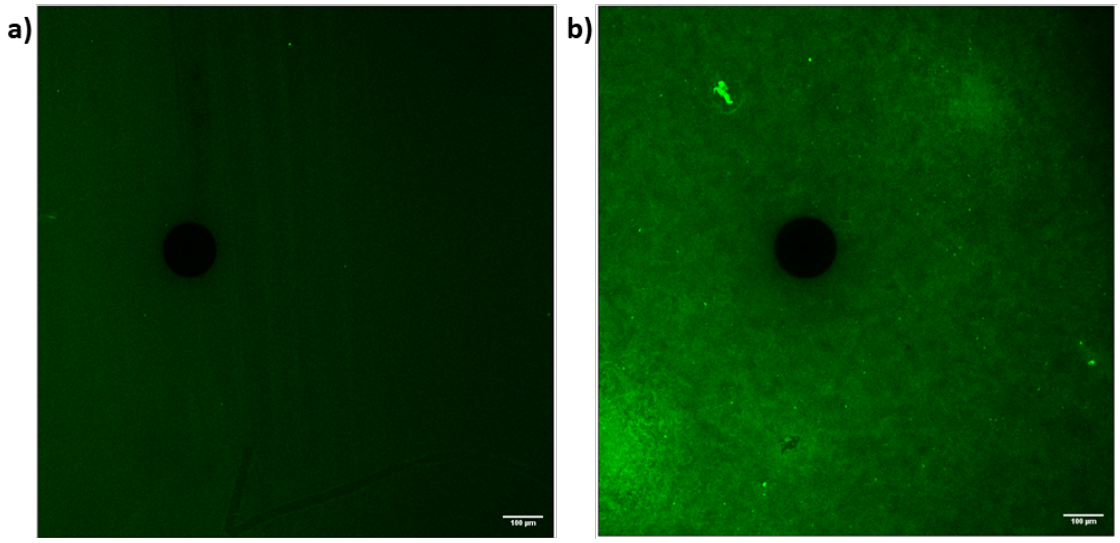

Figure S9. To ensure that the observed fluoresce is occurring due to the interaction between the SYBR Au and aptamers, a photobleaching step *i.e.*, photon-induced chemical damage to the dye to cause permanent loss of fluoresce (seen as a black circle) was performed on the a) poly-*D*-lysine (PDL)-aptamer-coated waveguide, and b) carbon nanotube (CNT)-PDL-aptamer-coated waveguide. The scale bar is 100 µm.

Table S1. Table with the histamine aptamer and scrambled control sequence where the number and type of nucleotides are conserved but the order changed.

	Composition (5' → 3')	A	C	G	T
Histamine aptamer	**ACG TGC GCC AGA GCG TAT ACC GTT GGA TGA TGG CCC GCG T**	7	11	14	8
Scrambled control	**CAA GTT CCT GGA GGG TCG ACG CAC GCG TAA CCG TGT GGC T**	7	11	14	8

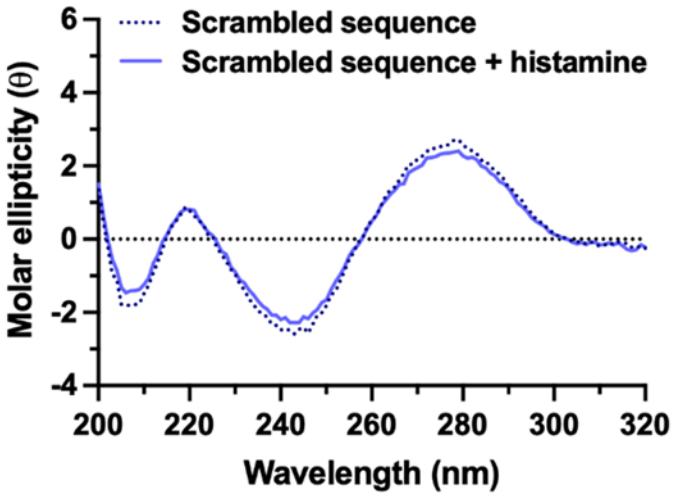

Figure S10. Circular dichroism spectroscopy of the control scrambled sequence upon incubation with histamine. Negligible changes in the spectra were observed.